Original Article

JOURNAL OF
biomaterials
applications

Journal of Biomaterials Applications
0(0) 1–9

DOI: 10.1177/0885328216669238
jba.sagepub.com

SAGE

Bio-printing cell-laden Matrigel–agarose constructs

Rong Fan[1,*], Marine Piou[1,*], Evan Darling[2], Denis Cormier[3], Jun Sun[4] and Jiandi Wan[1]

Abstract

3D printing of biological architectures that mimic the structural and functional features of *in vivo* tissues is of great interest in tissue engineering and the development of transplantable organ constructs. Printable bio-inks that are compatible with cellular activities play critical roles in the process of 3D bio-printing. Although a variety of hydrogels have been used as bio-inks for 3D bio-printing, they inherit poor mechanical properties and/or the lack of essential protein components that compromise their performance. Here, a hybrid Matrigel–agarose hydrogel system has been demonstrated that possesses both desired rheological properties for bio-printing and biocompatibility for long-term (11 days) cell culture. The agarose component in the hybrid hydrogel system enables the maintenance of 3D-printed structures, whereas Matrigel provides essential microenvironments for cell growth. When human intestinal epithelial HCT116 cells are encapsulated in the printed Matrigel–agarose constructs, high cell viability and proper cell spreading morphology are observed. Given that Matrigel is used extensively for 3D cell culturing, the developed 3D-printable Matrigel–agarose system will open a new way to construct Matrigel-based 3D constructs for cell culture and tissue engineering.

Keywords

3D printing, Matrigel, 3D tubular structures, 3D cell culture, human epithelial cells

Introduction

3D bio-printing has rapidly evolved as a "bottom-up" approach to fabricate complex biological constructs. Functional skin and cartilage, for example, have been fabricated using inkjet printing techniques where controlled deposition of cell-containing aqueous droplets on a substrate is used.[1–3] Laser-assisted printing, a nozzle-free technique that deposits droplets using focused laser pulses, enables high-resolution printing (30–100 μm) of cell-containing constructs and has been used to fabricate cellularized skin constructs.[4] Microextrusion, on the other hand, extrudes uninterrupted viscous bio-ink (up to 6×10^7 mPa/s) on substrates with a wide range of spatial resolutions (5 μm to millimeters) and therefore can fabricate tissue structures with complex geometries such as aortic valves,[5] branched vascular systems[6] and tumor models.[7]

Composition and material properties of the bio-ink play an essential role in printing techniques that were mentioned above. In addition to good biocompatibility, bio-inks must have suitable rheological properties suitable for printing. A rapid gelation process, for example, is required to maintain the stability of printed structures. Polysaccharide-based hydrogels such as alginate, hyaluronic acid and agarose have rapid gelation kinetics and proper mechanical properties for printing. Therefore, they have been used as bio-inks to print vessel-like structures,[8,9] porous constructs,[10,11] and aortic valve conduits.[5] However, polysaccharide-based hydrogel lack of essential protein components consequently have limitations with respect to cellular adhesion.[12] Protein-based hydrogels such as Matrigel contain necessary growth

[1]Microsystems Engineering, Rochester Institute of Technology, Rochester, NY, USA
[2]Department of Imaging and Photographic Technologies, Rochester Institute of Technology, Rochester, NY, USA
[3]Department of Industrial and Systems Engineering, Rochester Institute of Technology, Rochester, NY, USA
[4]Department of Medicine, University of Illinois at Chicago, Chicago, IL, USA
*These authors contributed equally to this work

Corresponding author:
Jiandi Wan, Microsystems Engineering, Rochester Institute of Technology, Rochester, NY, USA.
Email: jdween@rit.edu
Jun Sun, Medicine, University of Illinois at Chicago, Chicago, IL, USA.
Email: junsun7@uic.edu

factors and peptides and can facilitate cell growth and adhesion in 3D matrix.[13–16] Recently, Matrigel-based long-term culture systems have been developed for intestinal stem cells.[17,18] However, Matrigel, like the majority of protein-based hydrogels, has poor mechanical properties and is not suitable for printing,[19] which significantly limits its application as a bio-ink for 3D printing.

The goal of the present study is to develop hydrogels that not only support the growth of intestinal epithelial cells and cell–matrix interactions but also are 3D printable, and thus provide a proof-of-concept for 3D printing intestinal stem cells (ISCs). Because 3D printing is a bottom-up approach and provides fine spatial control over the position of cells along printed structures, 3D constructs that closely mimic the *in vivo* microenvironments of ISCs niche can be potentially produced via 3D printing. In addition, when different concentrations of growth factors are delivered via the printed 3D constructs, ISCs experience a spatiotemporal distribution of the growth factor and thus a spatially controlled organization of differentiated cell linage is expected. In this study, a hybrid Matrigel–agarose hydrogel system has been formed that is 3D printable and supports cell growth and cell–matrix interactions. Agarose is the material of choice due to its fast solidification rate upon printing and can maintain the printed structures in air. When human intestinal epithelial HCT116 cells were used as a model cell line and encapsulated in the printed Matrigel–agarose hydrogel, high cell viability and cell spreading morphology were observed. The proper combination of Matrigel with agarose therefore overcomes the disadvantages of individual hydrogels as bio-inks and provides a new type of bio-ink for 3D bioprinting and cell culturing.

Materials and methods

Cell maintenance

Human colonic epithelial HCT116 cells (ATCC) were cultured in a T-25 culture flask supplied with DMEM (Life Technologies) containing 10% (v/v) fetal bovine serum (FBS) (Life Technologies) and 1% (v/v) penicillin/streptomycin (Life Technologies) under 37°C and 5% CO_2. For preparation of the cell suspension, cells were washed by a PBS solution (Life Technologies) and treated by Trypsin (Life Technologies) for 5 min to detach them from the culture flask. The cell suspension was then centrifuged and re-dispersed in a fresh DMEM solution without adding FBS (1×10^8/ml) for further experimental use. Since dead cells were not attached on the culture flask and could be washed away by the PBS buffer during the washing step, the viability of cells in the suspension was approximately the same for all experiments.

Hydrogel preparation

Agarose stock solution was prepared by dissolving agarose powder (Sigma) in DI-water at 2 wt% or 3 wt%, and then homogenized and sterilized by boiling. The stock solution was then stored in an incubator at 37°C. Matrigel (50 μg/ml) (Corning) was stored at −18°C and pre-warmed overnight at 4°C before experimental use. To produce a gel mixture for 3D printing, agarose stock solution was first poured into a tube (Cristalgen) that had been pre-warmed at 37°C. Matrigel was then added by continuously mixing with a sterilized spatula, followed by the addition of cell suspension (1×10^8/ml). The gel mixture was homogenized by continuous stirring, and then transferred to the printing head of the 3D printer (Seraph Robotics) for printing or to the plate of a rheometer (Discovery Hybrid Rheometer, TA Instrument) for rheological testing.

Rheological measurement

The storage modulus (G′) and loss modulus (G″) of the hydrogel mixture at each concentration ratio were measured using a Discovery Hybrid Rheometer (TA Instrument) with a 40 mm diameter parallel plate. The measurements were conducted at room temperature and performed using six different angular frequencies from 1 to 10 rad/s. As soon as the Matrigel and agarose were mixed, the G′ and G″ of samples were measured every 3 min for 21 min.

3D bio-printing

A dual syringe 3D printer (Seraph Robotics) was used for the 3D bio-printing. The printing process was controlled by Seraph Print (Seraph). The programming code was written to design the shape of the printing structures point by point and imported to the Seraph Print software to be recognized by the printer. The 3D printer was sterilized with 70% ethanol before printing and was placed in a bio-cabinet to avoid contamination. During the printing process, a 0.9 mm diameter dispensing needle was used which produced printed line width on the order of 2 to 2.5 mm. The printing head was moved in x- and y-directions, and the platform was moved in z-direction. A motorized plunger inside the printing syringe continuously pushed the hydrogel out of the syringe. Hydrogel was printed layer by layer at a speed of 6 mm/s to build tubular structures in a collecting petri dish (Corning) or on glass slides (VWR) in air. The printed cell-laden tube was then filled with a DMEM culture medium and placed in an incubator at 37°C with a 5% CO_2 atmosphere for culturing. In order to facilitate microscopic imaging and observation of cell growth, some of the tubular structures were controlled at a height of 5 mm during printing.

All printing experiments without the syringe heater were conducted at room temperature and each printing cycle took approximately 20 min. Note that the initial temperature of agarose has to be kept at 37°C. This is due to agarose gelation process at temperature below 37°C, which results in blockage of the printing head. When the temperature is above 37°C, on the other hand, agarose solution has a relatively low viscosity, which compromises the printing resolution and 3D constructs. For 3D printing with temperature control, a syringe heater (New Era) was wrapped around the printing syringe and the temperature was maintained at 37°C during printing.

Determination of cell growth and cell viability

The growth and morphology of HCT116 cells cultured in hydrogel were examined using an inverted fluorescence microscope (Leica Microsystems, DMI 6000). Cell viability was determined using Live/Dead assays (Life Technologies) following the manufacture's protocol. To image cells encapsulated in the printed hydrogel, cells were stained with nucleus-blue (Life Technologies) and/or actin-green (Life Technologies) and imaged using a confocal microscope (Leica, TCS SP5). The percentage of cells that exhibited spreading-out morphologies was calculated by dividing the total number of cells counted each day with the number of spreading cells. Each set of experiments was repeated three times with at least 100 cells being counted for each experiment. Error bars are presented as the standard deviation of the mean.

Results

Printing 3D agarose structures and their cell viability

The printability of agarose was initially examined using a Seraph Robotics 3D printer. A circular pattern was designed by defining the coordinates of printing pathways in the Seraph Robotics code, which was then imported to the Seraph Print program to control the movement of the printing head. Then 2 wt% agarose solution heated at 37°C was loaded into the print head syringe, and was continuously extruded while printing (Figure 1(a)). By adjusting the tool path and the number of printed layers, tubular structures of agarose with a height of 5 cm, a wall thickness of 2 mm, and diameters of 12, 17, or 25 mm were printed (Figure 1(b)). By changing the design of printing patterns, tubular structures with star, triangle, and square morphology were constructed (Figure 1(c)). The highest tube printed using the current experimental setup was about 8 cm (online supplementary Figure S1).

We then printed agarose with encapsulated human HCT116 colonic epithelial cells to study the cell viability in such printed constructs. As shown in a 3D constructed confocal image of the tube (online supplementary Figure S2(a)), cells were dispersed throughout the entire structure of the agarose tube including the inner and outer surfaces. We found that cells were able to stay alive in the agarose tube after printing. However, the cell viability dropped rapidly to 35% after three days of culture (online supplementary Figure S2(c)). It was also observed that in contrast to the spindle-shaped cells cultured in protein-based

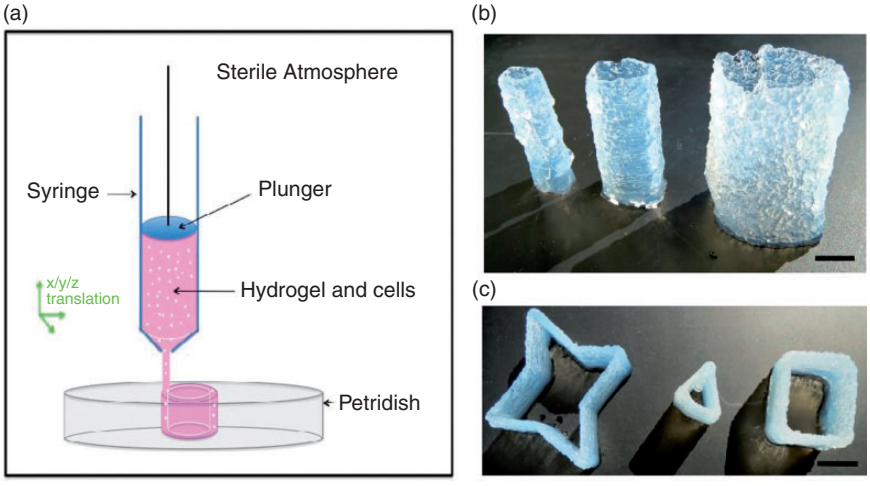

Figure 1. Experimental setup and representative images of 3D printed agarose constructs. (a) Schematic representation of the 3D printing setup. Cell-containing hydrogel loaded into a dispensing syringe in the printing head of a 3D printer is continuously extruded onto a petri dish in air. (b) 3D printed agarose tubes with different diameters (from left to right: $d = 12$, 17, and 25 mm) (scale bar = 10 mm). (c) 3D printed agarose constructs with a star, triangle, or square shape (scale bar = 8 mm).

hydrogels such as Matrigel,[20] cells growing in the agarose tube exhibit spherical morphology (online supplementary Figure S2(b)), indicating the lack of essential proteins that support cell attachment and spreading in agarose.[21]

3D printing Matrigel–agarose hybrid hydrogel

In order to improve cell growth and attachment in printed agarose constructs, we added Matrigel into the agarose matrix to form the Matrigel–agarose hybrid hydrogel. Agarose solidifies at temperatures below 32°C, whereas gelation of Matrigel occurs at temperatures above 4°C. The mixing of cold Matrigel with hot agarose solution therefore causes partial gelation of the hydrogel mixture immediately. We thus investigated the time-dependent change of the storage modulus (G′) and loss modulus (G″) of the agarose solution mixed with different volumetric fractions of Matrigel. Briefly, Matrigel was added to a 2 wt% agarose solution in volumetric ratios of 15%, 30%, or 50%. G′ and G″ as a function of time were then measured using a rheometer. As shown in Figure 2(a) and (b), increase of G′ and G″ with time was observed for all formulations. However, G′ was much larger than G″ and increased fourfold within 21 min, indicating that the mixed hydrogel became a more elastic-like polymer along gelation. When volumetric fractions of Matrigel increased from 15% to 50%, the value of G′ decreased, suggesting that adding Matrigel compromises the elastic property of the hybrid hydrogel. We further tested the printability of these hybrid hydrogels and found that 15% and 30% Matrigel possessed the desired mechanical properties ($G' > 1800$ Pa at 21 min) for printing (Figure S3(a) and (b)), whereas 50% Matrigel ($G' \sim 850$ Pa) failed to maintain the printed structure (online supplementary Figure S3(c)). Note that since the printing process was usually completed within 20 min, the rheological performance and printability of Matrigel–agarose hydrogels were examined within 21 min.

We further tested cell viability in the hybrid hydrogel with different volumetric factions of Matrigel. Our results showed that the percentage of spreading cells increased with the increase of volumetric factions of Matrigel (Figure 2(c)). When the volumetric factions were 15% and 30%, there were 9% and 23% of cells that exhibited spindle-like morphology after three days of culture (Figure 2(c)). Higher percentage of spreading cells (37%) was found when Matrigel fraction was 50%, which was consistent with a previous study of 3D colonoid culture in Matrigel.[13] Although hybrid hydrogel with 50% Matrigel supported more cells to spread and grow, it had poor printability due to the low G′ (Figures. 2(a) and S3(c)). In order to increase G′, the concentration of agarose stock solution was increased to 3 wt% while the volumetric faction of Matrigel was kept unchanged as 50%. As a result, a relatively high G′ (1250 Pa) of Matrigel–agarose hydrogel system was obtained. The hybrid hydrogel with 3 wt% agarose and 50% (v/v) Matrigel were then printed into a stable tubular structure with a diameter of 17 mm and a wall thickness of 2 mm (Figure 2(d)).

Therefore, human HCT116 cells were introduced to the tube composed of 3 wt% agarose and 50 v/v% Matrigel and culture the cells for 11 days. The results showed that, before day 8, the number of cells with spindle-like shape increased and that 72% of cells maintained spreading morphology (Figure 3(a)). Cells also tended to form clusters and spheroids (Figure 3(a) inset) after seeding, consistent with reported 3D cell culture in hydrogel.[22,23] The percentage of spreading cells, however, decreased from 70% to 47% between day 8 and day 11. Cell viability remained relatively high within the first six days (77%) but dropped after seven days (Figure 3(b)), which was consistent with the observed decrease of the percentage of spreading cells after day 8 (Figure 3(a)).

3D printing Matrigel–agarose hybrid hydrogel at constant temperature

Because printing was conducted at room temperature (25°C) whereas the initial temperature of the hybrid hydrogel was 37°C, the change of temperature along printing led to the change of rheological properties of the hybrid hydrogel with time (Figure 2). We thus tested whether the hybrid hydrogel could be printed at constant temperature (37°C). A syringe heater was used to wrap around the printing syringe and maintain the printing temperature at 37°C (Figure 4(a)). By repeating the printing process described above, a tubular structure with the same dimensions as the one printed without temperature control (a diameter of 17 mm and a wall thickness of 2 mm) was printed (Figure 4(b)). The tube printed at constant temperature was more transparent than that printed without temperature control (Figure 2(d)), probably due to a more homogeneous composition. When the tube was cut at its top, middle and bottom sections and examined under a microscope, no massive hydrogel clusters or granular structures were observed, indicating a relatively homogeneous composition (Figure 4(c)). Most importantly, when HCT116 cells were introduced to the hybrid hydrogel and printed at constant temperature (37°C), the percentage of spreading cells increased with culture time and reached 75% after 11 days of culturing (Figure 4(d)). Cell viability was also improved and maintained over 70% after 11 days of culturing, even though a slight decrease was found at the end of the culture (Figure 4(e)).

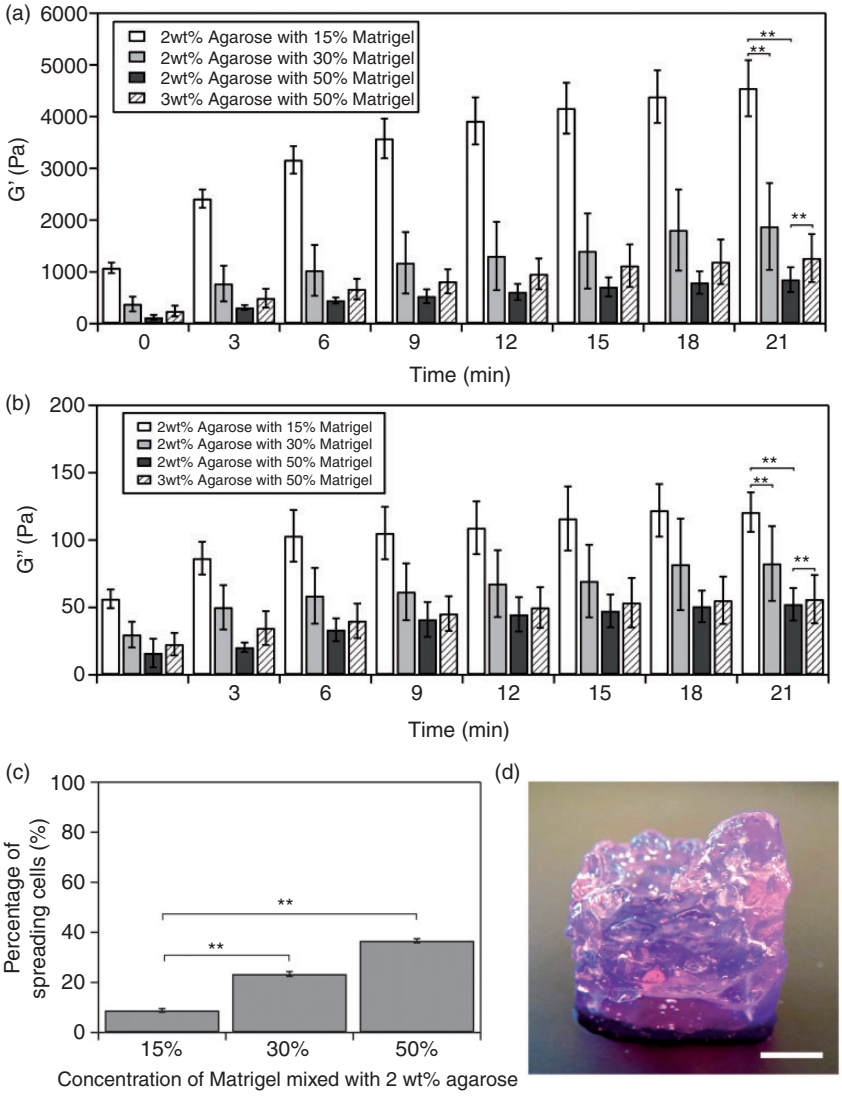

Figure 2. Characterization of Matrigel–agarose hybrid hydrogel. Dependence of the (a) storage modulus (G′) and (b) loss modulus (G″) of hybrid hydrogel on time at different compositions of Matrigel and agarose. $^{**}P < 0.01$ was calculated based on paired Student's *t*-test analysis. (c) Percentage of cells that exhibit spreading morphology after three days of culturing in 3D printed tubular structures composed of 2 wt% agarose and 15, 30, or 50% (v/v) Matrigel. $^{**}P < 0.01$ was calculated based on paired Student's *t*-test analysis. (d) An image of a 3D printed tubular structure using 50% (v/v) Matrigel and 3 wt% agarose. The tube has a diameter of 17 mm and a wall thickness of 2 mm (scale bar: 5 mm). Note that the purple color comes from the Matrigel and culture medium.

Discussion

In the current study, we developed Matrigel–agarose hybrid hydrogels and examined their rheological properties and 3D printability. Using human HCT116 cells in the printing hydrogels, cell growth and viability were evaluated. The desired mechanical properties of the hybrid hydrogel should first ensure a successful printing process and provide mechanical support for the printed structures. In addition, the mechanical properties of the hybrid hydrogel should not play a negative role in supporting cell growth. Furthermore, because Matrigel has been demonstrated for intestinal stem cells culture,[17,18] we expect the application of the developed hybrid Matrigel to benefit intestinal stem cells culture in 3D-printed structures. Hence, this can contribute to the construction of *in vivo*-mimicking intestinal model systems.

Agarose has feasible temperature-based gelation features and proper mechanical properties for 3D printing.[22,23] As a result, tubular structures that are consistent with previous studies[24] can be constructed and structures with star, triangle, and square morphology

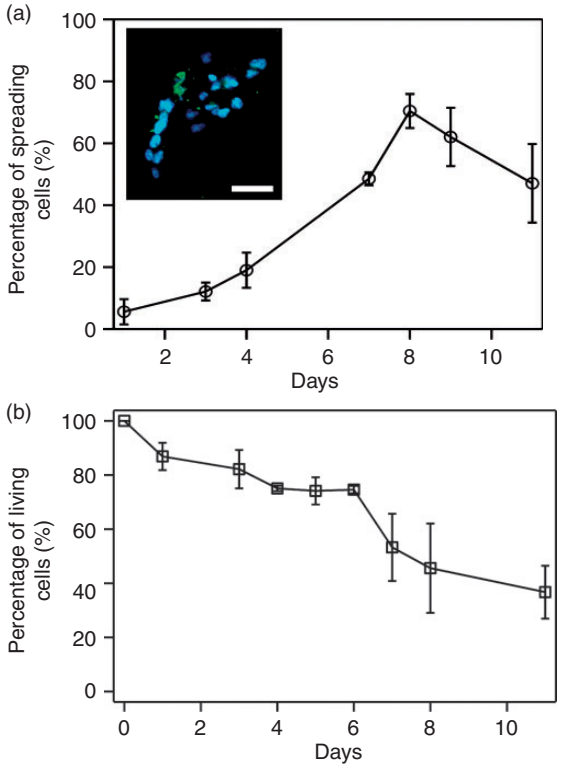

Figure 3. Cell growth in 3D printed Matrigel–agarose tubes composed of 3wt% agarose and 50% (v/v) Matrigel. (a) Percentage of cells that exhibit spreading morphology for 11 days of culturing. The percentage of spreading cells was calculated by dividing the total number of living cells with the number of spreading cells counted each day. Inset: A fluorescent confocal image of spreading cells and clusters formed in the printed tube. Cells are stained with actin-green and Nuc-blue (scale bar = 50 μm). (b) Cell viability over 11 days of culturing. The percentage of living cells was calculated by dividing the total number of cells with the number of living cells counted each day. Each set of experiments was repeated three times with at least 100 cells being counted for each experiment. Error bars are presented as the standard deviation of the mean.

are further demonstrated by 3D printing agarose (Figure 1). In addition, our study shows that tubular structures with a height of 8 cm (online supplementary Figure S1) can be achieved in air without the need of external structural support. In our experimental setup, agarose was loaded in the printing head at 37°C and cooled down during the printing process, which improved its elastic properties. As a result, agarose extruded from the printing head had enough mechanical strength to support the printed structure. However, it shall be noted that the printing process is accomplished within 20 min; otherwise, the gelation of agarose will block the printing head.

Agarose, however, lacks essential proteins to which cells can adhere and develop cell–matrix interactions.[12] HCT116 cells cultured in the printed agarose exhibited spherical morphology (online supplementary Figure S2) and failed to generate tensions against the 3D matrix to exhibit critical spindle-like morphology. This has been observed in protein-based hydrogels such as Matrigel and collagen.[20,25] When Matrigel was added into the agarose matrix, HCT116 cells started to spread out and the number of spreading cells increased with the increase of volumetric fractions of Matrigel (Figure 2(c)), indicating that adding Matrigel improves cell growth and adhesion in the 3D matrix. The percentage of spreading cells with spindle-like morphology in 50% Matrigel was 37% after three days of cell culturing. In fact, a previous study has shown that the growth of intestinal stem cells depends on the amount of Matrigel: the highest efficiency of colonoid formation ($33 \pm 5\%$) has been observed when 50% Matrigel is used.[13]

Adding excess Matrigel significantly affects the rheological performance and printability of agarose. It is known that when agarose solution (37°C) is placed at room temperature (25°C), G′ increases with time due to the gelation of agarose at low temperature.[26] This is consistent with what we observed here (Figure 2(a)). The temperature drop due to the addition of Matrigel (4°C) to agarose solution (37°C) did not increase the G′ of the hybrid hydrogel significantly; instead, G′ decreased with the increase of volumetric fractions of Matrigel. Since solidified Matrigel has a relative low G′ due to its high water content,[27] it is likely that adding Matrigel dilutes the hybrid hydrogel and compromises its elastic properties. Indeed, when the Matrigel–agarose was used to print tubes, 2 wt% agarose with 50% (v/v) Matrigel had the poorest printability (online supplementary Figure S3(c)). In order to increase the printability of Matrigel–agarose bio-ink while maintaining the high percentage of Matrigel to support cell growth and spreading, the concentration of agarose stock solution was increased to 3 wt% while Matrigel was kept constant at 50% (v/v). Because the volumetric fraction of Matrigel was kept constant, the increase of wt% of agarose did not affect the concentration of Matrigel in the mixture. The concentration of Matrigel in the hybrid hydrogel was 7.5, 15, and 50 μg/ml corresponding to 15%, 30%, and 50% (v/v) Matrigel, respectively. As a result, not only was G′ of 1250 Pa ($G'' \sim 60$ Pa) obtained for the hybrid hydrogel (Figure 2(a) and (b)) due to the increased wt% of agarose, but cell growth and cell–matrix interactions were improved. Stable tubular structure can therefore be printed and maintained (Figure 2(d)). Although previous studies have shown the development of hybrid hydrogel for 3D printing,[5,28] our study shows the correlation between the formulation of hybrid hydrogels with their rheological properties and biocompatibility, and hence provides quantitative understanding

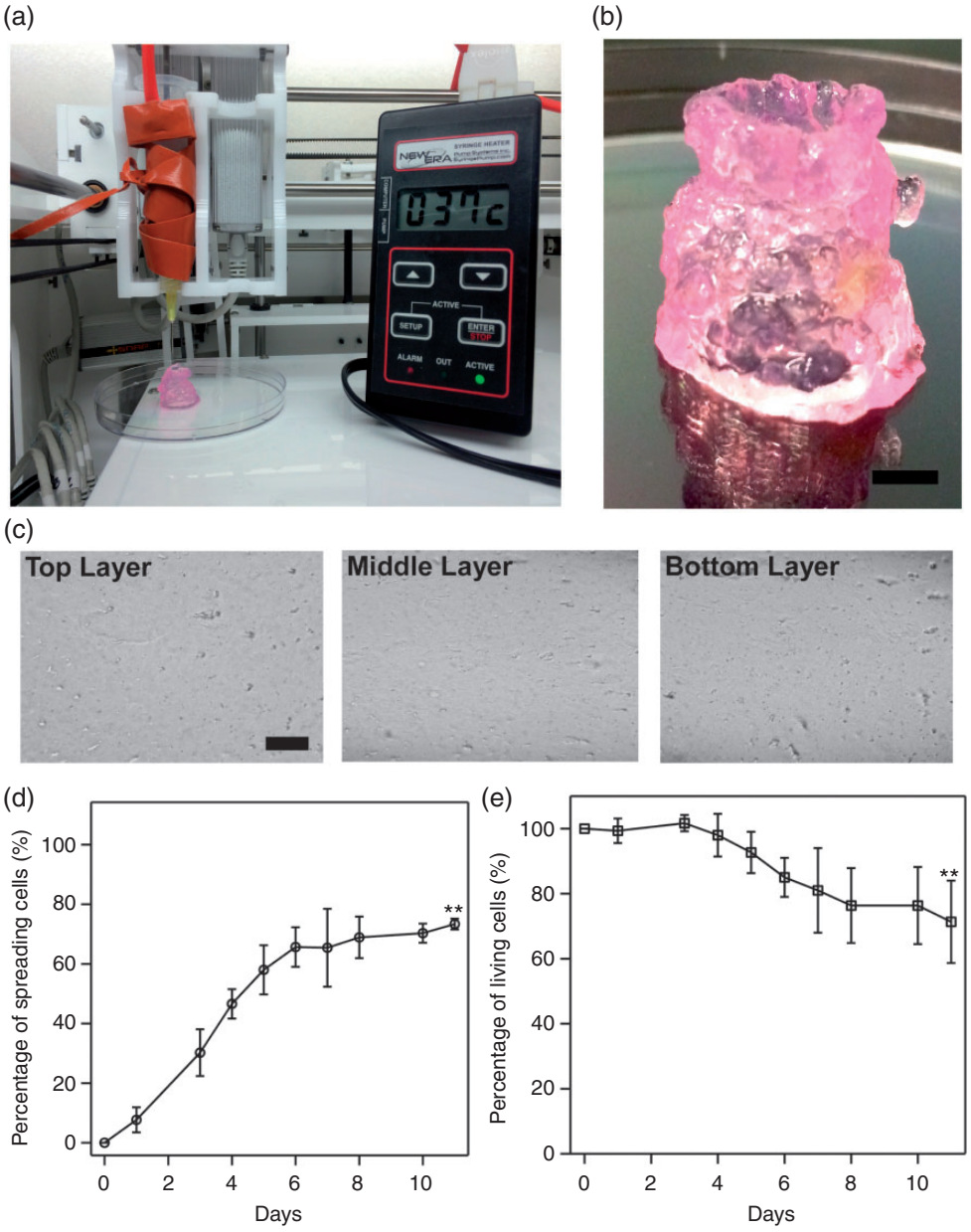

Figure 4. 3D printing Matrigel–agarose hybrid hydrogel at constant temperature (37 °C). (a) An image of the experimental setup in which a syringe heater was wrapped around the printing syringe to maintain the temperature at 37 °C during printing. (b) An image of 3D printed tubular structure composed of 3wt% agarose with 50% (v/v) Matrigel (scale bar: 5 mm). (c) Microscopic images of the 3D printed hybrid hydrogel tube cut at the top, middle, and bottom sections (scale bar: 100 μm). (d) Percentage of cells that exhibit spreading morphology for 11 days of culturing. (e) Cell viability over 11 days of culturing. $^{**}P < 0.01$ was calculated based on paired Student's *t*-test analysis between Figures 3(a) and 4(d), Figures 3(b) and 4(e), respectively.

of the material properties and biological activities of hybrid hydrogels for 3D bio-printing.

The results of culturing of HCT116 cells in 3D printed hydrogel constructs show that cells can spread and exhibit stretched non-spherical morphology during culture (Figure 3), indicating that the matrix supports cell adhesion and growth and cell–matrix interactions are established. However, a decrease of cell viability and reduced percentage of spreading cells in the late stage of culture was observed, which may arise from the heterogeneous structures of the tube when printed without temperature control. Because temperature of the hybrid hydrogel decreased with time, agarose would solidify during printing resulting in granular and non-uniform microstructures in the printed tube (Figures 1 and S1). The heterogonous structure could

render various physical properties such as stiffness at different locations of the tube and affect cellular behavior and direct cell fate.[29–31] In fact, our results show improved percentage of spreading cells and cell viability when cells are printed in more homogenous hybrid hydrogels. This indicates that homogeneous hydrogel matrix is supportive for cell growth and spreading. Note that it is also possible that the relative high modulus ($G' \sim 1250$ Pa) of the printed hybrid hydrogel negatively affects cell viability.[32–34] In addition, the diffusion length of oxygen and nutrient in hydrogel is around 150–200 μm,[35] whereas the wall thickness of the tube is 2 mm. Although the entire hydrogel tube is immersed in a culture medium during cell culture, it is likely that the cells had insufficient uptake of nutrients and oxygen through the tube wall. Our results thus highlight the much needed strategies for the development of physiologically relevant biomaterials and construction of vascular systems for 3D cell culture and tissue engineering, as shown by many recent efforts including results from our laboratory.[6,36,37]

Conclusion

In summary, we have demonstrated an approach to develop Matrigel–agarose hybrid hydrogels with desired rheological properties for 3D bio-printing and culturing human intestinal epithelial cells. The elasticity of the hybrid hydrogels increases with gelation time but decreases when the volumetric concentration of Matrigel increases. An optimized formulation of hybrid hydrogel with 50% (v/v) Matrigel and 3 wt% agarose was identified to be 3D printable and showed the ability to support cell growth and adhesion. In addition, both cell spreading and cell viability were significantly improved when printing was performed at a constant temperature (37°C). Therefore, the study provides useful guidelines to develop Matrigel-based hydrogels for 3D printing and tissue engineering.

Acknowledgement

The authors thank Hyla Sweet for her help on confocal microscopy and Caroline Kruse and Jack Smith for their help on the setup and programming on the 3D printer. They also thank Kanika Vats for her help on rheology measurements.

Authors' Contributions

RF and MP contributed equally to this work.

Declaration of conflicting interests

The author(s) declared no potential conflicts of interest with respect to the research, authorship, and/or publication of this article.

Funding

The authors gratefully acknowledge the support from the Rochester Institute of Technology. This work was partially supported by grants from NIDDK and Swim Across America Cancer Research Award to Jun Sun. Grant number: 1R01DK105118-01.

References

1. Cui X, Breitenkamp K, Finn M, et al. Direct human cartilage repair using three-dimensional bioprinting technology. *Tissue Eng Part A* 2012; 18: 1304–1312.
2. Skardal A, Mack D, Kapetanovic E, et al. Bioprinted amniotic fluid-derived stem cells accelerate healing of large skin wounds. *Stem Cells Trans Med* 2012; 1: 792.
3. Tan Y, Richards DJ, Trusk TC, et al. 3D printing facilitated scaffold-free tissue unit fabrication. *Biofabrication* 2014; 6: 024111.
4. Michael S, Sorg H, Peck C-T, et al. Tissue engineered skin substitutes created by laser-assisted bioprinting form skin-like structures in the dorsal skin fold chamber in mice. *PloS ONE* 2013; 8: e57741.
5. Duan B, Hockaday LA, Kang KH, et al. 3D bioprinting of heterogeneous aortic valve conduits with alginate/gelatin hydrogels. *J Biomed Mater Res A* 2013; 101: 1255–1264.
6. Norotte C, Marga FS, Niklason LE, et al. Scaffold-free vascular tissue engineering using bioprinting. *Biomaterials* 2009; 30: 5910–5917.
7. Xu F, Celli J, Rizvi I, et al. A three-dimensional in vitro ovarian cancer coculture model using a high-throughput cell patterning platform. *Biotechnol J* 2011; 6: 204–212.
8. Skardal A, Zhang J and Prestwich GD. Bioprinting vessel-like constructs using hyaluronan hydrogels crosslinked with tetrahedral polyethylene glycol tetracrylates. *Biomaterials* 2010; 31: 6173–6181.
9. Bertassoni LE, Cardoso JC, Manoharan V, et al. Direct-write bioprinting of cell-laden methacrylated gelatin hydrogels. *Biofabrication* 2014; 6: 024105.
10. Khalil S and Sun W. Bioprinting endothelial cells with alginate for 3D tissue constructs. *J Biomech Eng* 2009; 131: 111002.
11. Fedorovich NE, Wijnberg HM, Dhert WJ, et al. Distinct tissue formation by heterogeneous printing of osteo- and endothelial progenitor cells. *Tissue Eng Part A* 2011; 17: 2113–2121.
12. Awad HA, Wickham MQ, Leddy HA, et al. Chondrogenic differentiation of adipose-derived adult stem cells in agarose, alginate, and gelatin scaffolds. *Biomaterials* 2004; 25: 3211–3222.
13. Ahmad AA, Wang Y, Gracz AD, et al. Optimization of 3-D organotypic primary colonic cultures for organ-on-chip applications. *J Biol Eng* 2014; 8: 1.
14. Lu Y-C, Song W, An D, et al. Designing compartmentalized hydrogel microparticles for cell encapsulation and scalable 3D cell culture. *J Mater Chem B* 2015; 3: 353–360.
15. Radotra B and McCormick D. Glioma invasion in vitro is mediated by CD44–hyaluronan interactions. *J Pathol* 1997; 181: 434–438.

16. Tibbitt MW and Anseth KS. Hydrogels as extracellular matrix mimics for 3D cell culture. *Biotechnol Bioeng* 2009; 103: 655–663.
17. Sato T and Clevers H. Growing self-organizing mini-guts from a single intestinal stem cell: mechanism and applications. *Science* 2013; 340: 1190–1194.
18. Zhang YG, Wu S, Xia Y, et al. Salmonella-infected crypt-derived intestinal organoid culture system for host-bacterial interactions. *Physiol Rep* 2014; 2: e12147.
19. Wells RG. The role of matrix stiffness in regulating cell behavior. *Hepatology* 2008; 47: 1394–1400.
20. Gelain F, Bottai D, Vescovi A, et al. Designer self-assembling peptide nanofiber scaffolds for adult mouse neural stem cell 3-dimensional cultures. *PloS ONE* 2006; 1: e119.
21. O'Connor SM, Stenger DA, Shaffer KM, et al. Survival and neurite outgrowth of rat cortical neurons in three-dimensional agarose and collagen gel matrices. *Neurosci Lett* 2001; 304: 189–193.
22. Lang S, Sharrard R, Stark M, et al. Prostate epithelial cell lines form spheroids with evidence of glandular differentiation in three-dimensional Matrigel cultures. *Br J Cancer* 2001; 85: 590.
23. Takayama K, Kawabata K, Nagamoto Y, et al. 3D spheroid culture of hESC/hiPSC-derived hepatocyte-like cells for drug toxicity testing. *Biomaterials* 2013; 34: 1781–1789.
24. Campos DFD, Blaeser A, Weber M, et al. Three-dimensional printing of stem cell-laden hydrogels submerged in a hydrophobic high-density fluid. *Biofabrication* 2012; 5: 015003.
25. He J, Zhu L, Liu Y, et al. Sequential assembly of 3D perfusable microfluidic hydrogels. *J Mater Sci: Mater Med* 2014; 25: 2491–2500.
26. Xiong J-Y, Narayanan J, Liu X-Y, et al. Topology evolution and gelation mechanism of agarose gel. *J Phys Chem B* 2005; 109: 5638–5643.
27. Iyer N, Cooper K, Yang J, et al. Measuring elastic properties of thin biological films using capillary wrinkling. *AIP Conf Proc* 2008; 1042: 41–43.
28. Hong S, Sycks D, Chan HF, et al. 3D printing of highly stretchable and tough hydrogels into complex, cellularized structures. *Adv Mater* 2015; 27: 4035–4040.
29. Lutolf MP, Gilbert PM and Blau HM. Designing materials to direct stem-cell fate. *Nature* 2009; 462: 433–441.
30. Luo Y and Shoichet MS. A photolabile hydrogel for guided three-dimensional cell growth and migration. *Nat Mater* 2004; 3: 249–253.
31. Huebsch N, Arany PR, Mao AS, et al. Harnessing traction-mediated manipulation of the cell/matrix interface to control stem-cell fate. *Nat Mater* 2010; 9: 518–526.
32. Balgude A, Yu X, Szymanski A, et al. Agarose gel stiffness determines rate of DRG neurite extension in 3D cultures. *Biomaterials* 2001; 22: 1077–1084.
33. Pek YS, Wan AC and Ying JY. The effect of matrix stiffness on mesenchymal stem cell differentiation in a 3D thixotropic gel. *Biomaterials* 2010; 31: 385–391.
34. Ehrbar M, Sala A, Lienemann P, et al. Elucidating the role of matrix stiffness in 3D cell migration and remodeling. *Biophys J* 2011; 100: 284–293.
35. Liu J, Hilderink J, Groothuis TA, et al. Monitoring nutrient transport in tissue-engineered grafts. *J Tissue Eng Regen Med* 2015; 9: 952–960.
36. Fan R, Sun Y and Wan J. Leaf-inspired artificial microvascular networks (LIAMN) for three-dimensional cell culture. *RSC Adv* 2015; 5: 90596–90601.
37. Miller JS, Stevens KR, Yang MT, et al. Rapid casting of patterned vascular networks for perfusable engineered three-dimensional tissues. *Nat Mater* 2012; 11: 768–774.